Virus-induced translational arrest through 4EBP1/2-dependent decay of 5′-TOP mRNAs restricts viral infection

Kaycie C. Hopkins[a,1], Michael A. Tartell[a], Christin Herrmann[a], Brent A. Hackett[a], Frances Taschuk[a], Debasis Panda[a], Sanjay V. Menghani[a], Leah R. Sabin[b], and Sara Cherry[a,2]

[a]Department of Microbiology, University of Pennsylvania School of Medicine, Philadelphia, PA 19104; and [b]Watson School of Biological Sciences, Cold Spring Harbor Laboratory, Cold Spring Harbor, NY 11724

Edited by Michael J. Gale, Jr., University of Washington School of Medicine, Seattle, WA, and accepted by the Editorial Board April 20, 2015 (received for review October 6, 2014)

The mosquito-transmitted bunyavirus, Rift Valley fever virus (RVFV), is a highly successful pathogen for which there are no vaccines or therapeutics. Translational arrest is a common antiviral strategy used by hosts. In response, RVFV inhibits two well-known antiviral pathways that attenuate translation during infection, PKR and type I IFN signaling. Despite this, translational arrest occurs during RVFV infection by unknown mechanisms. Here, we find that RVFV infection triggers the decay of core translation machinery mRNAs that possess a 5′-terminal oligopyrimidine (5′-TOP) motif in their 5′-UTR, including mRNAs encoding ribosomal proteins, which leads to a decrease in overall ribosomal protein levels. We find that the RNA decapping enzyme NUDT16 selectively degrades 5′-TOP mRNAs during RVFV infection and this decay is triggered in response to mTOR attenuation via the translational repressor 4EBP1/2 axis. Translational arrest of 5′-TOPs via 4EBP1/2 restricts RVFV replication, and this increased RNA decay results in the loss of visible RNA granules, including P bodies and stress granules. Because RVFV cap-snatches in RNA granules, the increased level of 5′-TOP mRNAs in this compartment leads to snatching of these targets, which are translationally suppressed during infection. Therefore, translation of RVFV mRNAs is compromised by multiple mechanisms during infection. Together, these data present a previously unknown mechanism for translational shutdown in response to viral infection and identify mTOR attenuation as a potential therapeutic avenue against bunyaviral infection.

translational arrest | 5′-TOP mRNA | RNA decay | Rift Valley fever virus | RNA granule

As obligate intracellular parasites with limiting coding capacity, viruses must use host complexes and pathways to replicate. One hijacked pathway is the host translational machinery; all viruses depend on ribosomes for the translation of their mRNAs. This dependency has led to the evolution of translational arrest as a robust antiviral mechanism (1, 2). PKR inhibits global translation through the phosphorylation of a major factor in translation initiation, EIF2A. Phosphorylation of EIF2A stabilizes the EIF2–EIF2B–GDP complex, thereby inhibiting the GTP exchange and Met-tRNA$_i^{MET}$ binding required for further rounds of translation initiation (2, 3). Furthermore, type I interferons (IFNs), which are rapidly induced during many viral infections, lead to the induction of a large panel of IFN-stimulated genes (ISGs), including IFIT proteins, which inhibit translation initiation at multiple steps (1). To counter these mechanisms, many viruses overcome or subvert these responses, including via the inhibition of PKR and IFN signaling. Furthermore, viruses can bypass these mechanisms by accessing the translational apparatus using noncanonical approaches such as the internal ribosome entry sites of flaviviruses, such as hepatitis C virus, which bypasses requirements for many translation initiation factors (4).

In addition to inhibiting viral infection, translational arrest is a conserved cellular mechanism to cope with diverse cellular stressors, including chemical and environmental challenges (5). Although global changes in protein synthesis or RNA decay are regulated, increasing evidence suggests that there is also specificity, in that functionally related mRNAs can be synchronously regulated at the level of translation or RNA stability (6, 7). Coordinated changes in the translation and stability of cohorts of genes have been linked to specific RNA-binding proteins and conserved *cis* elements within the untranslated regions (UTRs) (6). These "RNA operons" have been well-established for some classes of genes, including cell cycle-regulated replicating histone mRNAs, controlled by the levels of stem-loop binding protein (SLBP) (8). In immunity, the RNA binding proteins ELAV/Hu and TTP target chemokine and cytokine mRNAs and alter their stability (6), and the half-lives of these RNAs are synchronously regulated during immune responses (6). Furthermore, evidence in yeast demonstrates that the individual components of complexes, including the ribosome, have incredibly similar mRNA half-lives (7), suggesting coordinate regulation of their stability. As much of the modulation of gene expression occurs

Significance

Rift Valley fever virus (RVFV), a mosquito-transmitted bunyavirus, blocks the two common methods of antiviral translational shutdown, PKR and type I interferon. However, it has previously been shown that RVFV infection halts protein production in infected human cells. Here, we demonstrate that RVFV is restricted by a previously unknown mechanism of antiviral translational shutdown, wherein 5′-terminal oligopyrimidine (5′-TOP) mRNAs encoding the core translational machinery are selectively degraded by the RNA decapping enzyme NUDT16 during RVFV infection, and that this decay is triggered in response to mTOR attenuation via the translational repressor 4EBP1/2 axis. We present a previously unknown mechanism for translational shutdown in response to viral infection and identify mTOR attenuation as a potential therapeutic target against bunyaviral infection.

Author contributions: K.C.H. and S.C. designed research; K.C.H., M.A.T., C.H., B.A.H., F.T., D.P., and S.V.M. performed research; L.R.S. contributed new reagents/analytic tools; K.C.H., M.A.T., C.H., B.A.H., F.T., D.P., S.V.M., and L.R.S. analyzed data; and K.C.H. and S.C. wrote the paper.

The authors declare no conflict of interest.

This article is a PNAS Direct Submission. M.J.G. is a guest editor invited by the Editorial Board.

[1]Present address: Division of Infectious Diseases and Vaccinology, School of Public Health, University of California, Berkeley, CA 94720.

[2]To whom correspondence should be addressed. Email: cherrys@mail.med.upenn.edu.

This article contains supporting information online at www.pnas.org/lookup/suppl/doi:10.1073/pnas.1418805112/-/DCSupplemental.

posttranscriptionally, these downstream regulatory mechanisms have the advantage of a specific and rapid response to stimuli.

Arthropod-borne viruses (arboviruses) are a subset of viruses that are transmitted from arthropods (typically a mosquito or tick) to mammals; to productively infect such disparate hosts, these viruses have adapted to use highly conserved pathways while evading the immune responses of both hosts. The mosquito-transmitted bunyavirus Rift Valley fever virus (RVFV) is a highly successful pathogen: it has developed evasion strategies that lead to the inhibition of PKR activity (9) and blocks the activation of type I IFNs (10). Furthermore, RVFV gains access to host ribosomes by "cap-snatching" the 5′ ends of host mRNAs. During viral mRNA transcription in the cytoplasm, host mRNA caps are recognized by the viral nucleocapsid protein (N) and cleaved 10–18nt downstream of the 5′ cap by the viral polymerase (L), which has endonuclease activity (11–14). This capped oligomer is then used as the primer for viral transcription. By masking its 5′ ends using endogenous caps, RVFV evades host pattern recognition receptors (PRRs) while efficiently accessing host ribosomes (15). It is thought that cap-snatching occurs within cytoplasmic RNA granules known as processing bodies (P bodies): RVFV N associates with P bodies in insect cells, and another bunyavirus, Sin Nombre virus, localizes to P bodies in human cells (16, 17).

Here, we find that RVFV infection leads to global shutdown of translation through the specific decay of the core translational machinery, including ribosomal protein mRNAs. A feature of these translationally related mRNAs, including the core translation machinery, is the presence of 5′-terminal oligopyrimidine (5′-TOP)–containing sequence at the extreme 5′ terminus of their mRNAs (18–20). This motif is conserved (21) and has been defined as a 5′-terminal cytosine followed by four pyrimidines (18, 19, 22). Recent work demonstrated that this classical 5′-TOP motif definition may be too strict, as mRNAs containing 5′-TOP–like motifs (mRNAs containing a series of five pyrimidines beginning within four bases of the 5′ end) behave similarly to bona fide 5′-TOP–containing mRNAs in regard to regulation of their translation (23). Previous studies showed that these 5′-TOP mRNAs are translationally regulated by mTOR signaling and its downstream target 4EBP which inhibits cap-dependent translation by binding to the translation initiation factor eIF4E (23, 24). Upon attenuation of mTOR signaling, these mRNAs are no longer associated with polysomes and are relocalized to stress granules (25), where mRNAs are translationally stalled but not degraded (26). Indeed, mTOR inhibition is not sufficient to decrease the stability of these mRNAs. We find that RVFV infection leads to the attenuation of mTOR signaling, activating 4EBP to inhibit translation, and under these conditions also induces the decay of 5′-TOP mRNAs. This suggests that viral infection sends two complementary signals. The first leads to mTOR attenuation, relocalizing 5′-TOP mRNAs to stress granules where their translation is stalled, and the second signal sends these mRNAs for degradation in P bodies, where the decapping and other RNA decay machinery resides. Although there are two well-characterized decapping enzymes, we found that NUDT16 selectively targets 5′-TOP mRNAs for decay. We also found that there is a second consequence to this induced decay: because RVFV cap-snatching machinery resides in P bodies, the virus snatches 5′-TOP mRNAs, thus making these viral mRNAs less suitable for translation. Altogether, these data suggest that coordinate decay of 5′-TOP mRNAs attenuates translation at multiple levels and restricts RVFV infection.

Results

RVFV Induces 5′-TOP mRNA Loss. Although it has been demonstrated that RVFV infection inhibits protein production during infection of mammalian cells (27), the mechanism is unknown as RVFV inhibits the two canonical antiviral pathways that block translation in response to viral infection, PKR and IFN (9, 10). Previous reports have demonstrated that the translation of 5′-TOP mRNAs is inhibited in response to a variety of stresses including attenuation of mTOR signaling (25), thus inhibiting global translation because many 5′-TOP mRNAs encode the translation machinery. Therefore, we examined whether RVFV infection impacted the basal levels of a panel of endogenous 5′-TOP–containing mRNAs during infection. We found a greater than twofold decrease in the levels of 5′-TOP–containing mRNAs 24 h after RVFV infection in U2OS cells, a human osteosarcoma cell line that is permissive to RVFV infection (Fig. 1*A*). This decrease in 5′-TOP mRNAs was also reflected at the protein level, as immunoblot analysis showed decreased RPS3A and RPS8 protein expression upon RVFV infection (Fig. 1*B*). Levels of mRNAs lacking a 5′-TOP (Fig. S1*A*) and 28S rRNA remained stable in RVFV-infected cells (Fig. 1*A*). We confirmed that this was generalizable to other mammalian systems by infecting mouse embryonic fibroblasts (MEFs) with RVFV and observed decreased levels of 5′-TOP mRNAs and decreased protein levels upon infection (Fig. 1 *C* and *D*).

We next examined whether loss of 5′-TOP mRNAs was dependent on RVFV replication. We found no change in 5′-TOP mRNA levels in U2OS cells treated with UV-killed RVFV, whereas WT virus dramatically decreased RPS3A and RPS8 mRNA levels (Fig. 1*E*). Altogether, these results demonstrate that infection with replication-competent RVFV leads to the loss of 5′-TOP mRNAs accompanied by a decrease in the expression levels of the translation machinery.

5′-TOP mRNAs Have Decreased Stability During RVFV Infection. Next, we determined whether RVFV infection impacted transcription of 5′-TOP mRNAs or their stability. For these studies, we examined the decay rate of 5′-TOP mRNAs or mRNAs lacking a 5′-TOP during RVFV infection. Normally, ribosomal protein mRNAs are stable, with half-lives in the range of 12 h in mammals (28), which we hypothesized would be reduced upon infection. U2OS cells were infected with RVFV for 17 h, and then treated with actinomycin D (ActD) to inhibit mRNA transcription. Given the long half-lives of these mRNAs, total RNA was collected at 3-h intervals and analyzed by reverse transcription–quantitative real-time PCR (RT-qPCR). Although we observed little decay of RPL24 (Fig. 2*A*), RPS3A (Fig. 2*B*), or RPS8 (Fig. 2*C*) mRNA in uninfected cells treated with ActD over 9 h, all three mRNAs showed increased decay during RVFV infection ($P < 0.001$; Fig. 2 *A*–*C*). In contrast, there was no change in the decay rate of two mRNAs lacking a 5′-TOP (Fig. S1 *B* and *C*). Therefore, RVFV infection induces 5′-TOP mRNA decay, resulting in decreased 5′-TOP mRNA and protein levels during infection.

RVFV Inhibits 5′-TOP mRNA Translation Early in Infection, Followed by Global Translation Inhibition. We next sought to determine whether this decay was specific to mRNAs containing a 5′-TOP motif, and whether that motif was necessary and sufficient for RVFV-induced mRNA decay. Human U2OS cells were transfected with reporter constructs containing an EEF2 5′-UTR upstream of a luciferase reporter, encoding either its native 5′-TOP motif (TOP-WT) or a mutated 5′-TOP UTR (TOP-MUT) (23). Twenty-four hours after transfection, cells were infected with RVFV [multiplicity of infection (MOI), 5] for 16 h, and luciferase activity was analyzed. We found that luciferase activity from the WT 5′-TOP reporter was decreased upon infection similar to the endogenous 5′-TOPs. Furthermore, the MUT reporter was less sensitive to infection induced changes in translation, translating significantly more efficiently than the WT 5′-TOP during infection (Fig. 2*D*).

Because the loss of the core translation machinery due to the decay of 5′-TOP mRNAs (Fig. 1) should ultimately impact

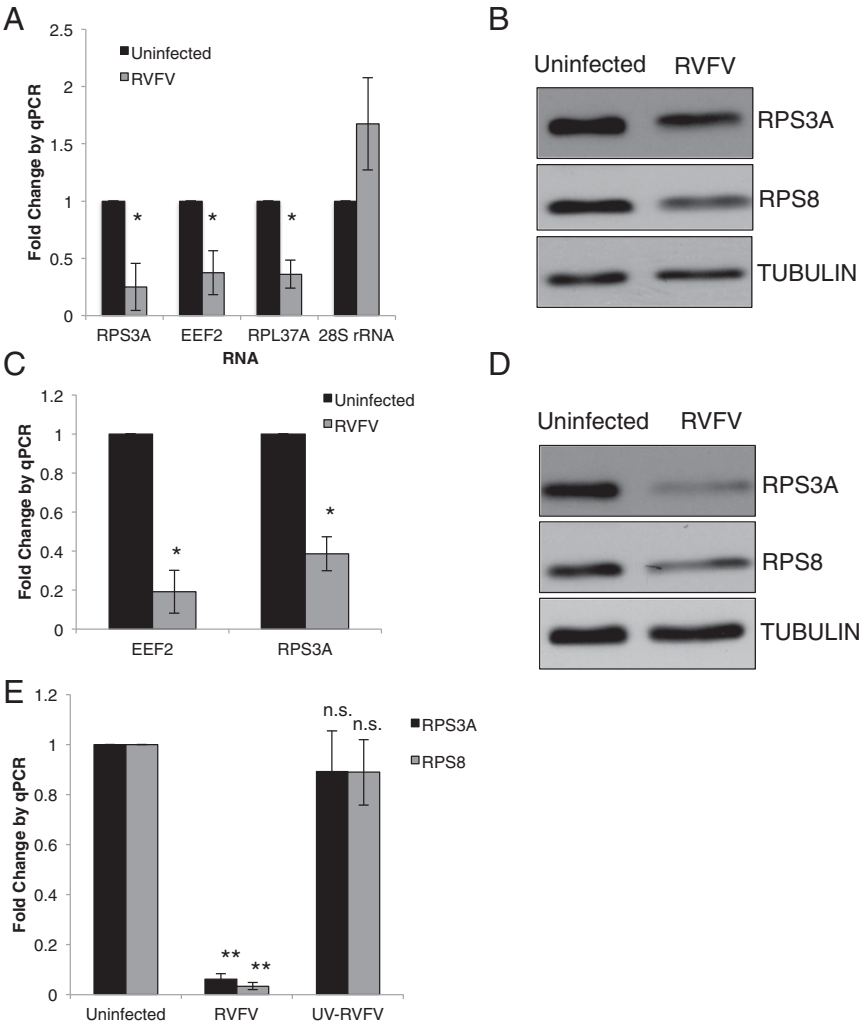

Fig. 1. RVFV infection leads to decreased 5′-TOP mRNA and ribosomal proteins. (*A*) U2OS cells were infected with RVFV (MOI, 2) for 24 h and total RNA was collected and analyzed by RT-qPCR. Fold change in 5′-TOP mRNA signal is indicated compared with uninfected U2OS cells as normalized to 28S rRNA with mean ± SD ($n = 3$; $^*P < 0.05$). (*B*) U2OS cells were treated as in *A*, and total protein was collected and analyzed by immunoblot. (*C*) Murine embryonic fibroblasts (MEFs) were infected with RVFV (MOI, 2) for 20 h, and total RNA was collected and analyzed by RT-qPCR. Fold change in 5′-TOP mRNA signal is indicated compared with uninfected MEFs as normalized to 28S rRNA with mean ± SD ($n = 3$; $^*P < 0.05$). (*D*) MEFs were infected with RVFV (MOI, 2) for 20 h; total protein lysate was collected and analyzed by immunoblot. (*E*) U2OS cells were infected with WT or UV-killed RVFV (MOI, 50–100) for 24 h, and total RNA was collected and analyzed by RT-qPCR. Fold change in RPS8 mRNA or RPS3A mRNA is indicated compared with uninfected U2OS cells as normalized to 28S rRNA with mean ± SD ($n = 3$; $^*P < 0.05$).

translation globally, as observed by Brennan et al. (27), we hypothesized that at later time points postinfection the translation of both 5′-TOP mRNAs and non–5′-TOP mRNAs would be similarly impacted. Therefore, we monitored translation from our reporters at a later time [24 h postinfection (hpi)] and found that translation of both the TOP-WT and TOP-MUT constructs were attenuated to the same degree during infection (Fig. 2*E*). Altogether, these data suggest that RVFV initially inhibits the translation of 5′-TOP mRNAs, subsequently leading to an inhibition of global protein translation.

RVFV Infection Attenuates mTOR Signaling and Activates 4EBP1. Recent studies have revealed that the translation of 5′-TOP–containing mRNAs is under the control of mTOR via the 4EBP1/2 axis (23). Translational efficiency of 5′-TOP mRNAs is inhibited by the ATP-competitive mTOR inhibitor Torin 1, which is dependent on the 5′-TOP mRNA *cis* element (23). Furthermore, we recently showed that RVFV infection attenuates Akt signaling (29), a known upstream activator of the mTORC1 complex. Therefore, we determined the activation status of the mTOR pathway, and in particular 4EBP1, during RVFV infection. We found that the mTOR pathway was attenuated during RVFV infection in MEFs: the phosphorylation status of Akt, and of two downstream targets of mTOR (RpS6 and 4EBP1) was reduced 18 hpi, whereas total levels were unaffected (Fig. 3*A*). This timing is coincident with a significant decrease in 5′-TOP mRNA and protein production (Fig. 1 *C* and *D*).

4EBP1/2 Is Required for 5′-TOP mRNA Decay and Controls RVFV Infection. mTOR regulates 5′-TOP mRNA translation through phosphorylation and inactivation of 4EBP1/2 (19, 23–25, 30, 31). Therefore, we hypothesized that RVFV-induced decay of 5′-TOP–containing mRNAs is dependent upon initial translational shutdown of these mRNAs via 4EBP1/2. To test this model, we obtained MEFs deficient in 4EBP1/2 [4EBP1/2 double knockout (DKO)] (23, 24) and examined the decay of 5′-TOP mRNAs during RVFV infection of WT or 4EBP1/2 DKO MEFs. We found that, at 20 hpi, although EEF2 and RPS3A mRNA levels both decreased in WT MEFs, no change was observed in these 5′-TOP–containing mRNAs in infected 4EBP1/2 DKO MEFs (Fig. 3*B*). This suggests that RVFV-induced decay of 5′-TOP mRNAs is 4EBP dependent and is likely preceded by the selective translational shutdown of these messages (Fig. 2*D*).

Translational shutdown is a common mechanism used by cells to restrict viruses (1, 2, 32), suggesting that the RVFV-triggered decay of 5′-TOP mRNAs and ribosomal proteins is a cellular response to inhibit RVFV infection. Therefore, we examined whether the loss of 4EBP1/2 impacted RVFV replication. Indeed, when we compared 4EBP1/2 mutant MEFs to their controls, we observed significantly increased viral infection as measured by microscopy (approximately fourfold; Fig. 3 *C* and *D*). Therefore, 4EBP1/2 controls both 5′-TOP translation and RVFV infection.

Although others have shown that direct mTOR inhibition leads to the translational arrest of 5′-TOP mRNAs (18, 22, 23),

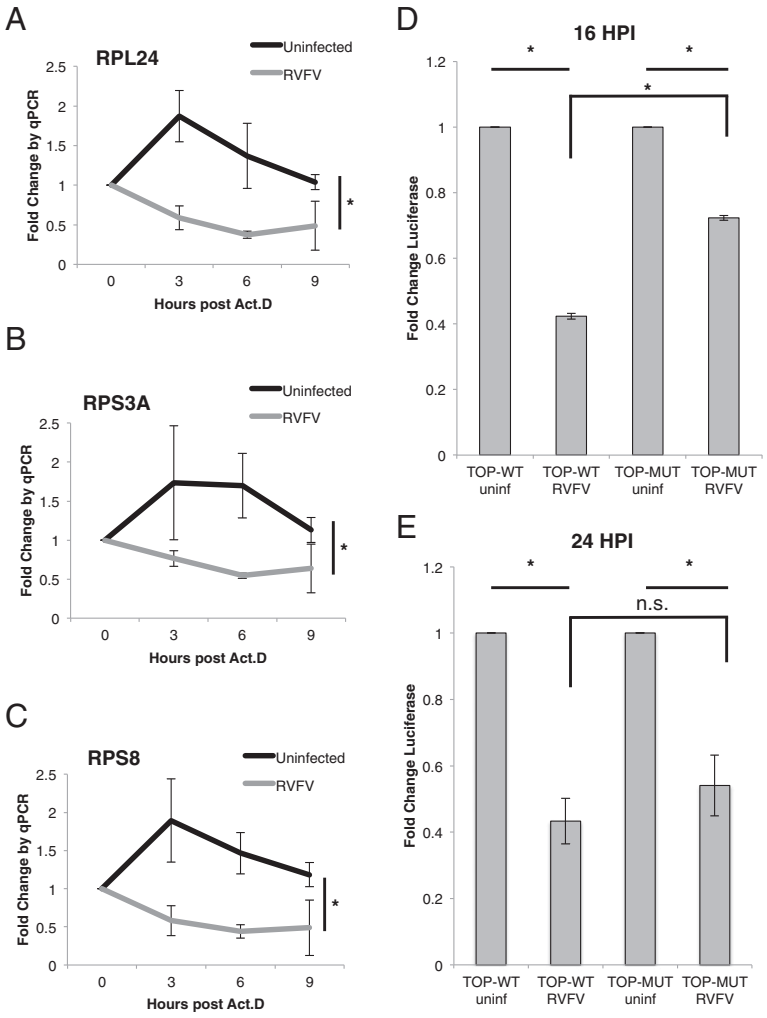

Fig. 2. RVFV induces 5′-TOP mRNA decay. (*A*–*C*) U2OS cells were infected with RVFV (MOI, 1) for 17 h, and then treated with ActD (5 μg/mL) for the indicated number of hours. Total RNA was collected at each time point and analyzed by RT-qPCR normalized to 28S rRNA for mean ± SD (n = 3). (*A*) 5′-TOP–containing RPL24 (*P = 0.0013). (*B*) 5′-TOP–containing RPS3A (*P = 0.0023). (*C*) 5′-TOP–containing RPS8 (*P = 0.0006). (*D* and *E*) U2OS cells were transfected with reporter constructs expressing either the WT TOP-containing EEF2 5′-UTR or a TOP-mutant UTR, and then untreated or infected with RVFV (MOI, 5). (*D*) Luciferase expression was measured 16 hpi. Mean ± SD is shown (n = 3; *P < 1E-3). (*E*) Luciferase expression was measured 24 hpi. Mean ± SD is shown (n = 3; *P < 0.05).

the decay of these mRNAs has not been observed. Therefore, we tested whether inhibition of mTOR was sufficient to induce decay of 5′-TOP mRNAs in our system. We found that treatment with the inhibitor Torin 1 (up to 24 h) had no impact on the levels of 5′-TOP–containing ribosomal protein mRNAs in MEFs (Fig. 3*E*), whereas RPS3A protein levels were decreased 18 h after Torin 1 treatment, consistent with previous reports (Fig. 3*F*) (23). Altogether, these data suggest that mTOR inhibition by RVFV leads to 4EBP1/2 activation which is necessary but not sufficient for RVFV-induced 5′-TOP mRNA decay. This suggests that a second virus-induced signal is required for 5′-TOP mRNA decay.

RNA Granules Are Regulated by RVFV Infection. To orchestrate RNA storage and RNA decay, the cell assembles RNA–protein complexes called RNA granules. There are two classical RNA granules that play interrelated roles in the cell: stress granules, which store translationally stalled mRNAs, and P bodies, which house the mRNA decay machinery where many mRNAs are decapped and degraded (26). These RNA granules are highly dynamic and tightly regulated; accumulation of mRNAs in these structures leads to the formation of visible punctae (33, 34), whereas increased RNA decay leads to their disaggregation without loss of activity (34). Furthermore, many diverse cellular insults cause stress granules to dock with and/or evolve into P bodies leading to the decay of resident RNAs (35, 36). Because 5′-TOP mRNAs have been shown to accumulate in stress granules upon inhibition of mTOR signaling (25), we reasoned that a RVFV-induced signal may lead to changes in these RNA granules, which would result in the decay of 5′-TOP mRNAs in P bodies. Therefore, we examined the architecture of RNA granules during RVFV infection by microscopy. We monitored these RNA granules in the presence and absence of infection using arsenic, which rapidly induces visible stress granules and P bodies (35). Within 30 min of arsenic treatment of U2OS cells, we observed a strong induction of stress granules using a panel of stress granule-associated proteins (G3BP, TIAR, and eIF4G) and P bodies using a panel of P-body–associated proteins (DCP1a, DCP2, and Rck/DDX6) (Fig. 4 *A* and *B*; quantified in Fig. S2*A*). However, in RVFV-infected cells, there was a significant loss of both stress granule and P-body punctae induction (Fig. 4 *A* and *B*; quantified in Fig. S2*A*). Furthermore, we found that this was cell autonomous, as only the infected cells lacked RNA granules (Fig. 4*C*).

The inability of RNA granules to form in RVFV-infected cells in response to arsenic treatment could indicate a specific defect; indeed, RNA granules can have differing protein composition depending upon the stimulus used for induction (35). Therefore, we tested whether RNA granules could be induced by other insults during RVFV infection. Cells were either mock treated or infected with RVFV for 12 h and exposed to heat shock or hydrogen peroxide. We found that Rck-containing granules were unable to form in response to either of these stimuli in infected

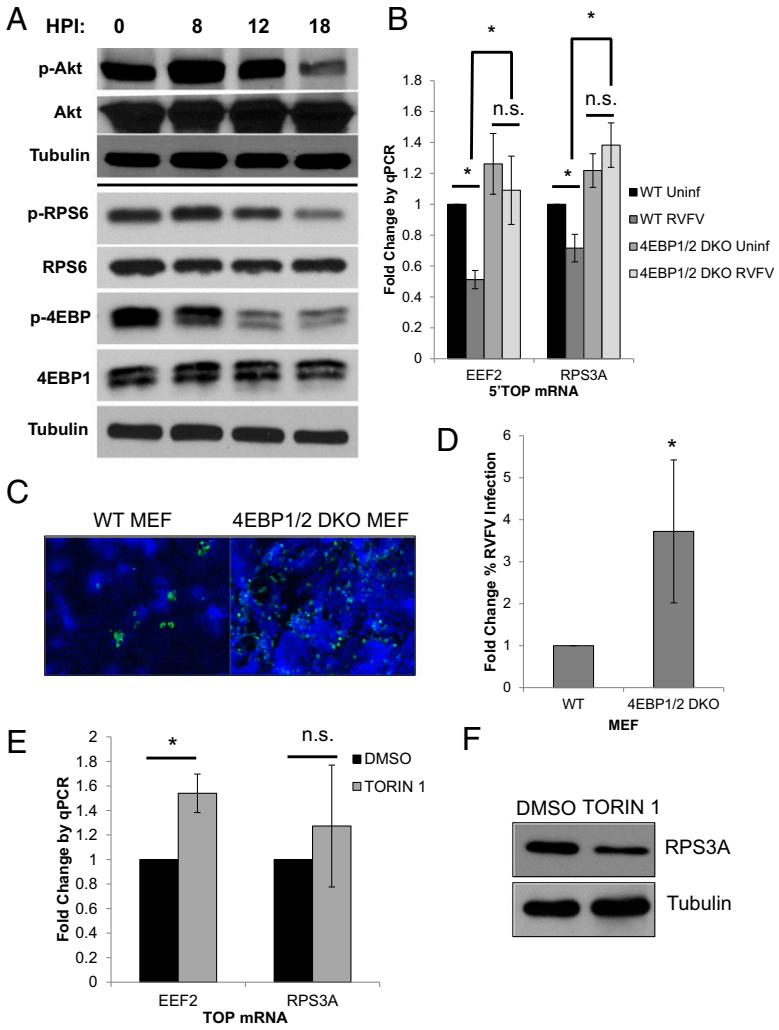

Fig. 3. 4EBP1/2 is required for RVFV-induced 5′-TOP mRNA decay. (*A*) MEF cells were infected with RVFV (MOI, 5) for the indicated time, and immunoblot analysis was performed. A representative of three independent experiments is shown. (*B*) WT or 4EBP1/2 double-knockout (DKO) MEFs were infected with RVFV (MOI, 2) for 20 h. Total RNA was collected and analyzed by RT-qPCR normalized to 28S rRNA. Mean ± SD is shown ($n = 3$; $^*P < 0.05$; n.s., not significant). (*C*) WT or 4EBP1/2 DKO MEFs were infected with RVFV (MOI, 0.04) and analyzed by microscopy (blue, nuclei; green, RVFV N), and the percentage of infected cells was quantified in *D* with mean ± SD shown ($n = 3$; $^*P < 0.05$). (*E*) WT MEFs were treated with DMSO or 250 nM Torin 1 for 24 h. Total RNA was collected and analyzed by RT-qPCR normalized to 28S rRNA. Mean ± SD is shown ($n = 3$; n.s., not significant). (*F*) WT MEFs were treated as in *D*, and total protein was analyzed by immunoblot. A representative of three independent experiments is shown.

cells, suggesting a general defect in RNA granule accumulation (Fig. S2 *B* and *C*) (35, 37).

RNA Granule-Resident Protein Levels Are Not Altered During RVFV Infection. The dispersal of RNA granules could be due to a loss of RNA granule-resident proteins required for assembly (38) or due to a loss in resident mRNAs necessary for nucleation (34). Indeed, P-body granule aggregation into visible punctae is not necessary for the decay functions that occur in P bodies, and increased mRNA decapping leads to the loss of visible P-body granules and continued RNA decay (33, 34). Additionally, translation complexes can be stalled in the absence of visible stress granules (39). Therefore, we first examined the steady-state levels of a panel of RNA granule-resident proteins during RVFV infection by immunoblot. We found no change in the levels of P-body proteins (DCP2, Rck/DDX6, or DCP1a) or stress granule proteins (TIAR, eIF4G, G3BP) in U2OS cells infected with RVFV at 8, 18, or 24 hpi compared with uninfected cells (Fig. 4*D*). These data, together with our data showing decreased stability of 5′-TOP mRNAs, suggest that the loss of visible RNA granules is likely due to RVFV-induced signals increasing mRNA decay activity.

RNA Granule Dispersal Is Sequential During RVFV Infection. If RNA granule disaggregation was indeed due to increased mRNA decay, we might expect that stress granules would be depleted before P bodies as the 5′-TOP mRNAs were sent from the stress granules to P bodies for degradation. Therefore, we explored the kinetics of RNA granule loss during RVFV infection. We treated cells with arsenic at 0, 4, 6, 8, 10, and 12 hpi and monitored RNA granule formation. These experiments revealed that the accumulation of stress granules was impacted before P bodies, as early as 6 hpi (Fig. 4 *E* and *F*). Although Rck punctae remained 6–8 hpi, there was a significant loss in TIAR punctae (Fig. 4*F*); additionally, we observed close proximity of those remaining stress granules and P bodies in infected cells at 6 hpi (see close apposition of red and green in Fig. 4*E*). This suggests that stalled translation complexes are first accumulated in stress granules as previously reported, and the RNA is subsequently shuttled to P bodies for degradation, made possible by their tight interaction (35). The order of disappearance of the punctae supports this directionality.

This led us to examine whether RNA granule dispersal was dependent on viral replication. To this end, we treated cells with UV-inactivated RVFV and observed no impact on arsenic-induced RNA granule accumulation (Fig. S2*D*), consistent with our observation that UV-inactivated RVFV is insufficient to trigger 5′-TOP mRNA decay (Fig. 1*E*), suggesting that the second signal that induces both RNA granule dispersal and 5′-TOP mRNA decay is replication dependent and occurs as early as 6 hpi.

NUDT16 Selectively Targets 5′-TOP mRNAs. We found that RNA granules are dispersed in a sequential manner, and because granule-resident proteins are not degraded during RVFV infection, this

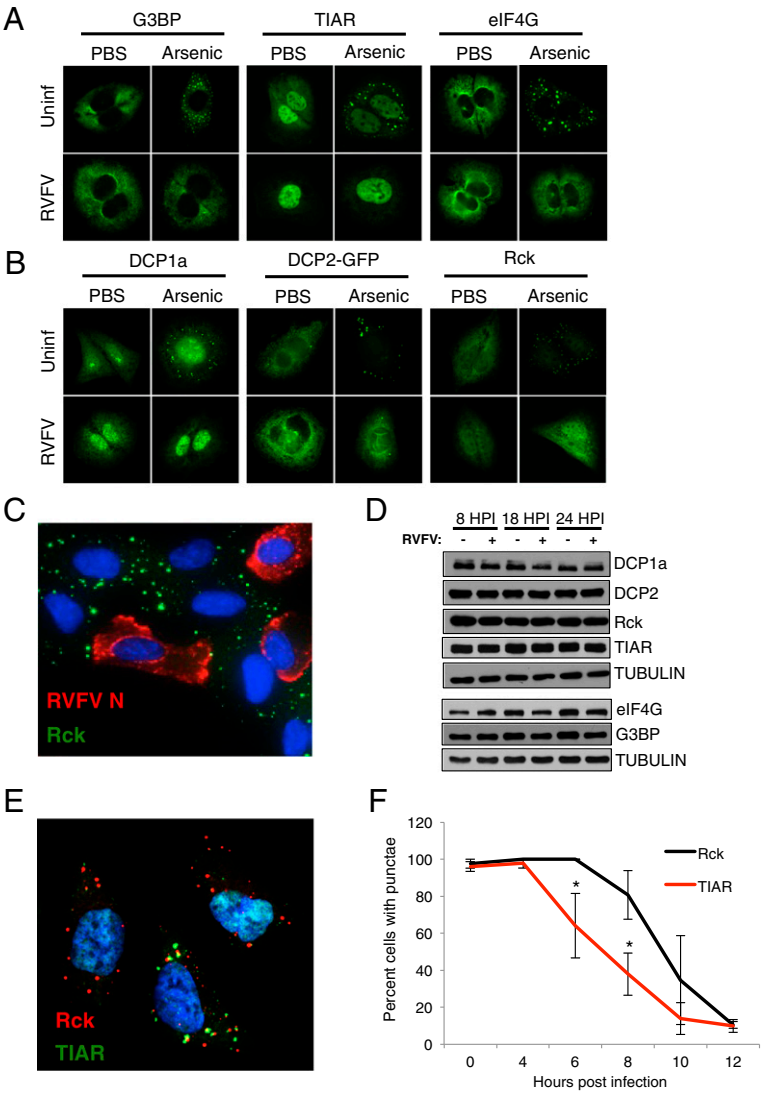

Fig. 4. RNA granules are disassembled during RVFV infection. (*A* and *B*) U2OS cells were mock treated or infected with RVFV (MOI, 10) for 12 h, and then treated with vehicle or 0.5 mM arsenic for 30 min and analyzed by microscopy for the indicated RNA granule-resident proteins. A representative of three independent experiments is shown (green, indicated protein) with stress granule proteins in *A* and P-body proteins in *B*. (*C*) U2OS cells were infected with RVFV (MOI, 1) for 12 h and analyzed by confocal microscopy. A representative of three independent experiments is shown (blue, nuclei; red, RVFV N; green, Rck/DDX6). (*D*) U2OS cells were infected for the indicated number of hours, and total protein lysates were collected and analyzed by immunoblot. A representative of three independent experiments is shown. (*E* and *F*) U2OS cells were infected with RVFV (MOI, 10) and processed for microscopy at the indicated time point postinfection and percent cells with either Rck or TIAR punctae was monitored. (*E*) Representative of three experiments at 6 hpi is shown (blue, nuclei; red, Rck; green, TIAR) and quantified in *F* with mean ± SD shown ($n = 3$; $*P < 0.05$).

suggests that decay of nucleating RNAs is responsible for the dispersal, consistent with the decreased stability of 5′-TOP mRNAs. Therefore, we next examined whether the P-body–resident RNA decapping machinery is involved (40). In mammals, there are two characterized decapping enzymes, the canonical decapping enzyme DCP2, and the more recently identified NUDT16 (41). The specific mRNA targets for these decapping enzymes are not completely understood; it is thought that they have both unique and overlapping targets (42–44). We examined whether the mRNA decapping enzymes DCP2 or NUDT16 control the levels of 5′-TOP mRNAs using the 5′-TOP luciferase reporters. We transiently expressed either Flag-tagged NUDT16 (41) or GFP-tagged DCP2 (45) (Fig. S3 *A* and *B*) and found that ectopic expression of either NUDT16 or DCP2 decreased levels of luciferase from 5′-TOP mRNAs (Fig. 5*A*, TOP-WT), suggesting that both decappers are limiting and can decay these substrates. Intriguingly, although enforced expression of DCP2 decreased luciferase levels from a mutant 5′-TOP reporter (TOP-MUT), increasing NUDT16 levels had no effect (Fig. 5*A*), suggesting specificity for this decapping enzyme. We also examined the effects of siRNA depletion of DCP2 and NUDT16 (Fig. S3 *C* and *D*) on luciferase reporters. In contrast to ectopic expression (Fig. 5*A*), DCP2 depletion did not affect luciferase expression of either the WT or mutant TOP reporter (Fig. 5*B*). However, NUDT16 depletion led to a specific increase in TOP-WT, but not TOP-MUT luciferase expression (Fig. 5*B*). Overall, these data suggest that 5′-TOP mRNAs are a selective target of NUDT16-dependent decay.

RVFV Cap-Snatches from 5′-TOP mRNAs. Data suggest that bunyaviruses cap-snatch mRNAs targeted to P bodies (16, 17). Therefore, we hypothesized that RVFV would cap-snatch 5′-TOP mRNAs targeted for degradation in infected human cells. We performed 5′-RACE to sequence the 5′ end of viral mRNAs and identified 119 snatched sequences that aligned with the human genome at 5′-UTRs (Table S1) (16). The mean length of endogenously cap-snatched sequences was 13.2 nt (SD, ±1.7) (Fig. S4*A*); this is consistent with previous reports that placed bunyaviral cap-snatching products between 10 and 18 nt (46). Informatic analysis suggested an overall preference for snatching endogenous host mRNAs with pyrimidines at their 5′ end, a signature of 5′-TOP mRNAs (Fig. S4 *B* and *C*). Gene Ontology enrichment analysis revealed that cap-snatched sequences were enriched for genes involved in mRNA translation ($P = 2E\text{-}24$; Fig. S4*D*), including mRNAs encoding core components of the translation machinery, such as protein components of the ribosome and translation initiation and elongation factors that contain 5′-TOPs (Table S1 and Fig. S4 *D* and *E*). As recent reports have shown that the classical 5′-TOP motif definition may be too strict, we included mRNAs

containing 5′-TOP–like motifs (mRNAs containing a series of five pyrimidines beginning within four bases of the 5′ end) in our analysis as they have been demonstrated to be regulated at the translational level identically to classical 5′-TOP–containing mRNAs (23). Previous reports have estimated that, in mice, based on well-annotated 5′-UTRs, ∼16% of mRNAs in the genome encode 5′-TOP or 5′-TOP–like motifs (23). We observed that greater than 35% of the mRNAs cap-snatched by RVFV in human cells contained 5′-TOP motifs and that this enrichment was highly significant (Fig. 5*C*, P = 1E-7). Indeed, we found many cap-snatched sequences were from canonical examples of 5′-TOP motifs (Fig. 5*D*). These data show that 5′-TOP–containing mRNAs are indeed targeted to P bodies, where the viral cap-snatching machinery incorporates them into viral mRNAs. The targeting of genes with this motif explains the observed bias toward pyrimidines at the 5′ end of snatched mRNAs (Fig. S4*B*).

Incorporation of 5′-TOP–Containing mRNA Caps into RVFV N mRNA Is Limited by NUDT16. Next, we examined whether the decapping enzymes may selectively impact the ability of RVFV to snatch 5′-TOP mRNA targets. Because NUDT16 had a selective preference for 5′-TOPs (Fig. 5 *A* and *B*), we reasoned that depletion of NUDT16 would lead to increased snatching of these targets. U2OS cells were depleted of either DCP2 or NUDT16 (Fig. S3 *C* and *D*), and infected with RVFV for 20 h, and total RNA was examined by RT-qPCR using a primer strategy to amplify specific host mRNAs that are cap-snatched (16). Briefly, a forward primer containing a linker followed by 10–18 bp of the extreme 5′ end of the indicated 5′-TOP–containing endogenous mRNA was used with a reverse primer specific for RVFV N RNA. Examination of a panel of seven 5′-TOP-RVFV N mRNA conjugate mRNAs revealed that siRNA depletion of NUDT16 led to at least a fivefold increase in the levels of all conjugates tested (Fig. 5*E*). Conversely, although DCP2 depletion led to an overall trend in increased TOP-N conjugates, only three were significant, and the increase was maximally threefold (Fig. 5*E*). This suggests that RVFV mRNA snatching of these 5′-TOP caps is limited by decapping and, when taken in combination with reporter assay results (Fig. 5 *A* and *B*), suggests that NUDT16 is the primary decapping enzyme for 5′-TOP mRNAs in human cells.

Discussion

We found a clear interplay between RVFV infection, mTOR signaling, and translational arrest via 5′-TOP mRNA decay, suggesting the model depicted in Fig. S5. During RVFV infection, recognition of a viral PAMP on the incoming virus serves

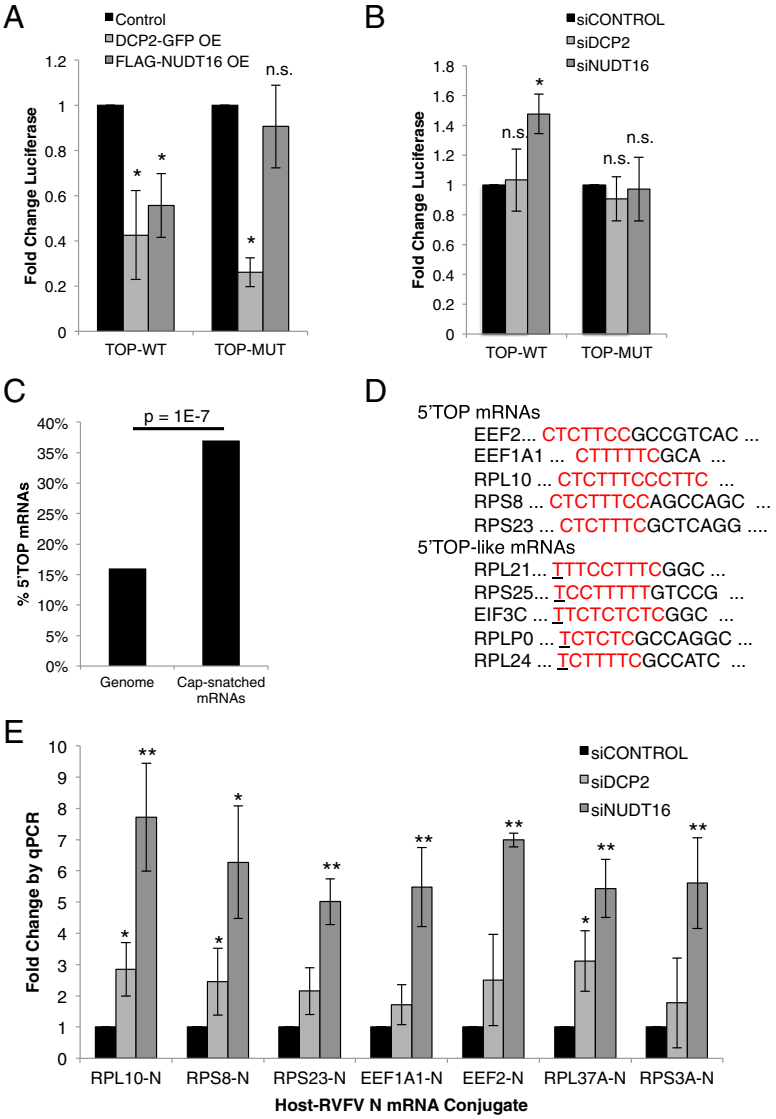

Fig. 5. 5′-TOP mRNAs targeted for decay are substrates for the competing cap-snatching and RNA decay machinery. (*A*) U2OS cells were transfected with reporter constructs expressing either the WT TOP-containing EEF2 5′-UTR or a TOP-mutant UTR, along with either control or DCP2-GFP or FLAG-NUDT16. Luciferase expression was measured by luminescence with mean ± SD shown (n = 3; *P < 0.05). (*B*) U2OS cells were transfected with the indicated siRNAs along with reporter constructs expressing either the WT-TOP or MUT-TOP luciferase construct. Luciferase expression was measured by luminescence, with mean ± SD shown (n = 3; *P < 0.05; n.s., not significant). (*C*) Percent of 5′-TOP–containing mRNAs in the mouse genome (*Left*) versus the proportion of 5′-TOP mRNAs snatched by RVFV in human U2OS cells (*Right*). P value was calculated using χ^2 test. (*D*) Example 5′-TOP or 5′-TOP–like mRNAs (red) in the dataset of 119 genes cap-snatched by RVFV. Full-length cap-snatched sequences are shown. (*E*) U2OS cells were treated with the indicated siRNAs and then infected with RVFV (MOI, 1). Total RNA was collected 20 hpi and analyzed by RT-qPCR for TOP- RVFV N mRNA conjugates. Fold change is normalized to 28S rRNA, with mean ± SD (n = 3; *P < 0.05, **P < 0.01).

as a signal to attenuate Akt–mTOR signaling (Fig. 3*A*) (29). This leads to increased 4EBP1/2 activity, inhibiting the translation of TOP mRNAs and sending them to stress granules (23). Because attenuation of the mTOR pathway is not sufficient for 5′-TOP decay (Fig. 3*E*), nor RNA granule dispersal (Fig. S2*E*), we suggest that viral infection produces a second signal that induces the relocalization of 5′-TOP mRNAs to sites where the decapping machinery is present, which then results in the decay of these 5′-TOP mRNAs and the loss in RNA granule architecture.

We suggest that the decay of 5′-TOP mRNAs during RVFV infection leads to the decreased ribosomal protein levels we observed in Fig. 1 *B* and *D*, as well as decreased protein levels of other 5′-TOP mRNAs, which include many translation initiation and elongation factors. This in turn results in decreased levels of global translation (Fig. 2*E*). The half-lives of the plethora of translation factors are not known, but it is known that ribosomal proteins are very stable when integrated into ribosomes, with half-lives on the order of days in some tissues (47). However, it has been demonstrated that newly translated ribosomal proteins in the nucleolus are in excess for ribosome biogenesis and that it is the levels of rRNA that are rate-limiting for ribosomal assembly; thus, ribosomal proteins that are not complexed are rapidly degraded (48). Despite the longevity of cytoplasmic ribosomes, even transient changes in 5′-TOP mRNA translation during circadian rhythm cycling impact global translation (49). Indeed, even a 20% reduction in overall translation is sufficient to impact the levels of relatively stable housekeeping genes (49), suggesting that the larger decreases we see in ribosomal protein levels during RVFV infection (Fig. 1 *B* and *D*) are sufficient to explain both the decreased levels of global translation we observe (Fig. 2*E*) and the ability of 4EBP1/2 to restrict RVFV infection (Fig. 3 *B*–*D*). We therefore suggest that the decay of 5′-TOPs results in ribosomal proteins and other translation factors becoming rate-limiting for translation, and that during RVFV infection global translation is attenuated due to this decay.

Because inhibition of mTOR is not sufficient to induce decay (Fig. 3*E*), we suggest that under conditions where mTOR signaling is attenuated in the absence of the second virus-induced signal, the 5′-TOP mRNAs are transiently sequestered into stress granules and can be subsequently returned to the pool of translating mRNAs once the stress has been alleviated. This potential ability to store and subsequently reuse translational mRNAs may be beneficial (28); regenerating core translation mRNAs would be energetically costly in situations of transient stress. Indeed, in yeast it has been observed that translational arrest due to external stressors generally leads to increased mRNA stability, allowing time for the cell to assess the stress before launching an appropriate gene program (50). During viral infection, which is a strong insult that can ultimately be destructive, 5′-TOP mRNA decay would result in a more permanent inhibition of translation and eventually lead to loss of cell viability. We observed changes in RNA granules at 6 hpi (Fig. 4*F*), suggesting that if viral infection is not overcome by this time point the cell will shut down translation through a more permanent mechanism, perhaps leading to the destruction of the virally infected cell. Although we did not observe any loss in cell number during our studies, others have observed RVFV-induced cell death at later time points (51). Indeed, translational arrest by other antiviral pathways including PKR and IFN also ultimately results in the death of virally infected cells to prevent the spread of the infection from the initial infected cell (52, 53).

5′-TOP mRNA degradation by the P-body–associated decay machinery would explain both the increased decay of these mRNAs and the increased cap-snatching of these mRNAs during infection, because RVFV competes with the decapping machinery for targets in these compartments (Fig. 5*E*). Altogether, these activities would result in a loss of 5′-TOP mRNAs, which would have two clear consequences. First, it would lead to decreased levels of the 5′-TOP mRNAs encoding the translational machinery, ultimately inhibiting global translation as ribosomal proteins and other translation factors become depleted, consistent with observations that RVFV-induced global translational shutoff is slow and occurs at late time points (27).

Second, this increased mRNA decay would result in the dispersal of visible RNA granules, while the mRNA degradation machinery remained active. P bodies require RNA moieties to nucleate and maintain their visible structural integrity, and this can be compromised by RNase treatment of cells or by driving RNA decay via ectopic expression of the decapping machinery (34, 39). Viral infections can lead to complex interactions with RNA granules (54, 55). Some viruses, including poliovirus, encode proteases that degrade protein components of RNA granules; loss of these nucleation factors impedes granule architecture (38). Other viruses use RNA granule proteins for their own replication; flaviviruses including West Nile virus, dengue virus, and hepatitis C virus bring nucleation factors to sites of replication, resulting in defects in stress granule and P-body assembly (56–58). Because we see no effects of RVFV infection on P-body or stress granule protein stability, and no relocalization or novel granule structures forming in infected cells, the dispersal of P bodies and stress granules by RVFV is through a different mechanism. In this case, sensing of RVFV infection leads to activation, rather than inhibition, of mRNA decay and the ultimate dispersal of RNA granules. Indeed, cellular mRNA decay is induced by γ-herpesviruses and the severe acute respiratory syndrome coronavirus, although it is generally thought that this is mediated by direct degradation of host mRNAs by viral proteins (55, 59–62). The decay of cellular mRNAs is thought to promote viral replication because this alleviates the competition between cellular mRNAs and viral mRNAs for the cellular translation machinery (55). In contrast, our data suggest that 5′-TOP mRNA decay hinders viral replication by attenuating translation.

Thus, incorporation of 5′-TOPs into viral mRNAs may impact the efficiency of viral mRNA translation in multiple ways. First, viral mRNAs containing a 5′-TOP may be sent to sites of decay and cap-snatching, attenuating their ability to be translated; indeed, studies have shown that bunyaviruses can snatch their own 5′ ends (63), suggesting that viral mRNAs may be retargeted to sites of viral cap-snatching. Second, 4EBP-dependent changes in the translation machinery will make these 5′-TOPs poor substrates for translation. Last, as 5′-TOP mRNAs encoding the translation machinery are degraded, global effects on the core translational machinery will inhibit overall protein synthesis, including that of viral mRNAs. 4EBP1/2 inhibits 5′-TOP translation through sequestering eIF4E, and the ability of eIF4E to bind eIF4G1 is necessary to form the eIF4F complex (64). Interestingly, another bunyavirus, the hantavirus Sin Nombre virus, compensates for changes in the translation initiation machinery, in particular eIF4F, by directly recruiting scanning ribosomes via its nucleocapsid protein (65). Therefore, it is possible that this function of the Sin Nombre nucleocapsid protein evolved as a means to circumvent the inhibitory action of 4EBP1/2. Whether RVFV or other bunyaviruses are also able to do this is unknown.

Our data also shed light on the interplay between cytoplasmic cap-snatching and the decay machinery. Although we found that RVFV snatches coregulated mRNAs in both insect and human hosts, the cohorts of genes are distinct. In human cells, the predominant group are 5′-TOP mRNAs, whereas in insects we found that cell cycle-related genes were targeted (16). This expands our knowledge of RNA regulation and coordinate regulation of RNA stability, defining another set of targets for the decapping machinery (44). Indeed, our data suggest that NUDT16 selectively degrades 5′-TOP mRNAs. Whether this is due to enzymatic specificity, compartmentalization of the enzymes, or differential use of cofactors is an open question.

Although many viral infections lead to attenuation of mTOR signaling (66, 67), it is unclear whether this is a more general antiviral response to infection. In particular, 4EBP1/2 promotes rather than restricts vesicular stomatitis virus, Sindbis virus, influenza virus, and encephalomyocarditis virus infection (24). Indeed, 4EBP1/2-deficient mice are generally refractory to RNA virus infection due to increased type I IFN responses, including higher expression of IRF-7 (24, 68). 4EBP1/2 also negatively regulates the translation of many innate immune effector mRNAs, until released by mTOR signaling (68). Altogether, these data suggest that the restriction of RVFV by 4EBP is specific and only possible because RVFV blocks IFN activity (10). Nevertheless, the discovery that mTOR lies at the heart of this antiviral mechanism against RVFV is therapeutically promising. There are no Food and Drug Administration (FDA)-approved vaccines or antiviral therapeutics to treat bunyaviral infections, whereas mTOR inhibitors are FDA approved and in use, especially for cancer treatments. Although rapamycin is the classical inhibitor, it does not block all mTOR functions. In contrast, ATP-competitive inhibitors, including Torin 1, have been shown to inhibit all mTORC1 functions, including the 4EBP1/2 axis of translational control (23, 69). Therefore, we hypothesize that mTOR ATP-competitive inhibitors would boost this anti-RVFV response and attenuate infection in three ways: first, through the activation of antiviral autophagy (29); second, by enforcing the incorporation of 5′-TOP UTRs into viral mRNAs during a period where they are translationally inhibitory; and third, by promoting and enforcing translational shutdown.

Experimental Procedures

Replicates and Statistical Analyses. All replicates shown are biological replicates. Error bars are SD from the mean of $n = 3$ or 4 independent biological replicates. Statistics are calculated using Student's unpaired t test with unequal variance, for all experiments other than the linear regression analysis in Fig. 2 *A–C* (see analysis below). Results were considered significant if $P < 0.05$.

Cells, Viruses, Antibodies, and Reagents. U2OS cells and MEFs were grown and maintained as previously described (70, 71). MP12 strain of RVFV was grown in Vero cells as described (72). Antibodies were obtained from the following sources: anti-GFP (Invitrogen), anti-tubulin (Sigma), anti-RVFV N ID8 and anti-RVFV Gn 4D4 (gifts from R. Doms, University of Pennsylvania, Philadelphia), anti-Rck/DDX6 (MBL), anti-RPS3A (Abcam; ab96524), anti-RPS8 (Abcam; ab13803), anti-DCP1a (Abcam; ab47811), anti-TIAR (BD Biosciences; BD610352), anti-eIF4G (Santa Cruz; sc-11373), and anti-G3BP (BD Biosciences; BDB611126). All other primary antibodies were from Cell Signaling: p-S6(S240/244) (catalog #2215), S6 (catalog #2317), 4EBP (catalog #9452), p-4EBP(T37/46) (catalog #2855), Akt (catalog #9272), and p-Akt(S473) (catalog #9271). Fluorescent secondary antibodies were obtained from Invitrogen, and HRP-conjugated antibodies were from Amersham. Additional chemicals were obtained from Sigma.

siRNA. U2OS cells were seeded on six-well plates in 2 mL of complete DMEM, and then transfected with the indicated siRNA using HiPerfect transfection reagent in OptiMEM at a final concentration of 20 nM. Two siRNAs were pooled for each gene targeted. Cells were incubated for 3 d and then infected as described. siRNAs were from Ambion; sequences are available in *SI Experimental Procedures*.

Plasmids. FLAG-NUDT16 plasmid was a gift from M. Kiledjian, Rutgers University, Piscataway, NJ. The following plasmids were obtained from Addgene: GFP-DCP2 (catalog #25031); TOP-WT (catalog #38235); and TOP-MUT (catalog #38236).

Reporter Assays. U2OS cells were transfected with 0.04 μg of TOP-WT or TOP-MUT plasmids (23) obtained from Addgene (38235 and 38236) and 0.96 μg of empty vector (pcDNA3.1+), FLAG-NUDT16, or GFP-DCP2 using Xtremegene 9 according to the manufacturer's instruction. Twenty-four hours posttransfection, cells were uninfected or infected with RVFV (MOI, 5) and harvested 16 or 24 h later. Luciferase expression was quantified using the *Renilla*-GLO Luciferase Assay System (Promega) according to the manufacturer's directions.

Immunofluorescence. For percent infection quantification, cells were fixed, processed, imaged by automated microscopy [at least three wells per condition at least three sites per well (ImageXpressMicro; 10×)] and subject to automated image analysis using MetaXpress as described (73).

For RNA granule analysis, U2OS cells were seeded on coverslips, infected with RVFV, fixed, and processed for fluorescent microscopy (Leica DMI 4000 B fluorescent microscope; 63×). Where indicated, cells were treated with 0.5 mM As_2O_3 to induce RNA granules, which were quantified by automated imaged analysis (MetaXpress granule module).

RNA Analysis. Total RNA was extracted as previously described (74). RT-qPCR was performed as previously described (75). Primer sequences are described in *SI Experimental Procedures*.

Immunoblot. Total protein was collected in RIPA buffer and analyzed by reducing SDS/PAGE gel as previously described (72). Representative blots from ≥3 experiments shown.

ActD Treatment. U2OS cells were infected with RVFV (MOI, 1) for 17 h then treated with ActD (5 μg/mL) for the indicated number of hours. Total RNA was collected at each time point and analyzed by RT-qPCR. Statistical significance was assessed by fitting a linear model to each decay curve with explanatory variables of experimental replicate, infection, and linear or squared time; only infection showed a significant effect by ANOVA at 19 df, $P < 0.001$.

5′-RACE and Cloning. 5′-RACE was performed using the FirstChoice RLM-RACE kit from Ambion according to the manufacturer's instruction. RT-PCR was performed as described (75) using primers specific for the 5′-RACE adaptor (forward) and RVFV N transcript (reverse), and gel purified (Qiagen) before ligation using TOPO TA cloning system (Invitrogen).

BOWTIE Analysis of Human 5′-RACE Sequences. Snatched sequences were mapped to the Hg19 genome with Bowtie, using a seed length of 12 and allowing zero mismatches. The resulting regions were intersected with the coordinates of annotated human 5′-UTRs, downloaded from University of California, Santa Cruz (Hg19). The 5′-UTRs were then manually inspected to verify the presence of the snatched sequence near the transcriptional start site. If multiple matches were present, distance from the annotated transcriptional start site was used to determine the more likely match.

ACKNOWLEDGMENTS. We thank M. Tudor and E. Schmidt for bioinformatic and statistical assistance; N. Sonenberg for WT and 4EBP1/2 DKO MEFs; K. Rausch, A. Yasunaga, R. Moy, J. Molleston, and other members of S.C.'s laboratory for technical support, advice, and helpful discussions; M. Kiledjian for the Flag-NUDT16 construct; and R. Doms and C. Schmaljohn for RVFV antibodies. S.C. is a recipient of the Burroughs Wellcome Investigators in the Pathogenesis of Infectious Disease Award. This work was supported by National Institutes of Health Grants R01AI074951, U54AI057168, and R01AI095500 (to S.C.), and T32 NS007180 (to K.C.H.).

1. Diamond MS, Farzan M (2013) The broad-spectrum antiviral functions of IFIT and IFITM proteins. *Nat Rev Immunol* 13(1):46–57.
2. Kaufman RJ (1999) Double-stranded RNA-activated protein kinase mediates virus-induced apoptosis: A new role for an old actor. *Proc Natl Acad Sci USA* 96(21): 11693–11695.
3. Wek RC, Jiang HY, Anthony TG (2006) Coping with stress: eIF2 kinases and translational control. *Biochem Soc Trans* 34(Pt 1):7–11.
4. Lancaster AM, Jan E, Sarnow P (2006) Initiation factor-independent translation mediated by the hepatitis C virus internal ribosome entry site. *RNA* 12(5):894–902.
5. Holcik M, Sonenberg N (2005) Translational control in stress and apoptosis. *Nat Rev Mol Cell Biol* 6(4):318–327.
6. Keene JD (2007) RNA regulons: Coordination of post-transcriptional events. *Nat Rev Genet* 8(7):533–543.
7. Wang Y, et al. (2002) Precision and functional specificity in mRNA decay. *Proc Natl Acad Sci USA* 99(9):5860–5865.
8. Marzluff WF, Wagner EJ, Duronio RJ (2008) Metabolism and regulation of canonical histone mRNAs: Life without a poly(A) tail. *Nat Rev Genet* 9(11):843–854.
9. Ikegami T, et al. (2009) Rift Valley fever virus NSs protein promotes post-transcriptional downregulation of protein kinase PKR and inhibits eIF2alpha phosphorylation. *PLoS Pathog* 5(2):e1000287.
10. Billecocq A, et al. (2004) NSs protein of Rift Valley fever virus blocks interferon production by inhibiting host gene transcription. *J Virol* 78(18):9798–9806.

11. Mir MA, Sheema S, Haseeb A, Haque A (2010) Hantavirus nucleocapsid protein has distinct m7G cap- and RNA-binding sites. *J Biol Chem* 285(15):11357–11368.
12. Patterson JLJ, Holloway B, Kolakofsky D (1984) La Crosse virions contain a primer-stimulated RNA polymerase and a methylated cap-dependent endonuclease. *J Virol* 52(1):215–222.
13. Reguera J, Weber F, Cusack S (2010) Bunyaviridae RNA polymerases (L-protein) have an N-terminal, influenza-like endonuclease domain, essential for viral cap-dependent transcription. *PLoS Pathog* 6(9):e1001101.
14. Simons JF, Pettersson RF (1991) Host-derived 5′ ends and overlapping complementary 3′ ends of the two mRNAs transcribed from the ambisense S segment of Uukuniemi virus. *J Virol* 65(9):4741–4748.
15. Daffis S, et al. (2010) 2′-O methylation of the viral mRNA cap evades host restriction by IFIT family members. *Nature* 468(7322):452–456.
16. Hopkins KC, et al. (2013) A genome-wide RNAi screen reveals that mRNA decapping restricts bunyaviral replication by limiting the pools of Dcp2-accessible targets for cap-snatching. *Genes Dev* 27(13):1511–1525.
17. Mir MA, Duran WA, Hjelle BL, Ye C, Panganiban AT (2008) Storage of cellular 5′ mRNA caps in P bodies for viral cap-snatching. *Proc Natl Acad Sci USA* 105(49): 19294–19299.
18. Meyuhas O (2000) Synthesis of the translational apparatus is regulated at the translational level. *Eur J Biochem* 267(21):6321–6330.
19. Jefferies HB, Reinhard C, Kozma SC, Thomas G (1994) Rapamycin selectively represses translation of the "polypyrimidine tract" mRNA family. *Proc Natl Acad Sci USA* 91(10): 4441–4445.
20. Iadevaia V, Caldarola S, Tino E, Amaldi F, Loreni F (2008) All translation elongation factors and the e, f, and h subunits of translation initiation factor 3 are encoded by 5′-terminal oligopyrimidine (TOP) mRNAs. *RNA* 14(9):1730–1736.
21. Avni D, Biberman Y, Meyuhas O (1997) The 5′ terminal oligopyrimidine tract confers translational control on TOP mRNAs in a cell type- and sequence context-dependent manner. *Nucleic Acids Res* 25(5):995–1001.
22. Tang H, et al. (2001) Amino acid-induced translation of TOP mRNAs is fully dependent on phosphatidylinositol 3-kinase-mediated signaling, is partially inhibited by rapamycin, and is independent of S6K1 and rpS6 phosphorylation. *Mol Cell Biol* 21(24): 8671–8683.
23. Thoreen CC, et al. (2012) A unifying model for mTORC1-mediated regulation of mRNA translation. *Nature* 485(7396):109–113.
24. Colina R, et al. (2008) Translational control of the innate immune response through IRF-7. *Nature* 452(7185):323–328.
25. Damgaard CK, Lykke-Andersen J (2011) Translational coregulation of 5′TOP mRNAs by TIA-1 and TIAR. *Genes Dev* 25(19):2057–2068.
26. Thomas MG, Loschi M, Desbats MA, Boccaccio GL (2011) RNA granules: The good, the bad and the ugly. *Cell Signal* 23(2):324–334.
27. Brennan B, Welch SR, Elliott RM (2014) The consequences of reconfiguring the ambisense S genome segment of Rift Valley fever virus on viral replication in mammalian and mosquito cells and for genome packaging. *PLoS Pathog* 10(2):e1003922.
28. Sharova LV, et al. (2009) Database for mRNA half-life of 19 977 genes obtained by DNA microarray analysis of pluripotent and differentiating mouse embryonic stem cells. *DNA Res* 16(1):45–58.
29. Moy RH, et al. (2014) Antiviral autophagy restricts Rift Valley fever virus infection and is conserved from flies to mammals. *Immunity* 40(1):51–65.
30. Constantinou C, Elia A, Clemens MJ (2008) Activation of p53 stimulates proteasome-dependent truncation of eIF4E-binding protein 1 (4E-BP1). *Biol Cell* 100(5):279–289.
31. Elia A, Constantinou C, Clemens MJ (2008) Effects of protein phosphorylation on ubiquitination and stability of the translational inhibitor protein 4E-BP1. *Oncogene* 27(6):811–822.
32. Mohr I, Sonenberg N (2012) Host translation at the nexus of infection and immunity. *Cell Host Microbe* 12(4):470–483.
33. Teixeira D, Sheth U, Valencia-Sanchez MA, Brengues M, Parker R (2005) Processing bodies require RNA for assembly and contain nontranslating mRNAs. *RNA* 11(4): 371–382.
34. Eulalio A, Behm-Ansmant I, Schweizer D, Izaurralde E (2007) P-body formation is a consequence, not the cause, of RNA-mediated gene silencing. *Mol Cell Biol* 27(11): 3970–3981.
35. Kedersha N, et al. (2005) Stress granules and processing bodies are dynamically linked sites of mRNP remodeling. *J Cell Biol* 169(6):871–884.
36. Parker R, Sheth U (2007) P bodies and the control of mRNA translation and degradation. *Mol Cell* 25(5):635–646.
37. Emara MM, et al. (2012) Hydrogen peroxide induces stress granule formation independent of eIF2α phosphorylation. *Biochem Biophys Res Commun* 423(4):763–769.
38. Dougherty JD, White JP, Lloyd RE (2011) Poliovirus-mediated disruption of cytoplasmic processing bodies. *J Virol* 85(1):64–75.
39. Kedersha N, et al. (2000) Dynamic shuttling of TIA-1 accompanies the recruitment of mRNA to mammalian stress granules. *J Cell Biol* 151(6):1257–1268.
40. van Dijk E, et al. (2002) Human Dcp2: A catalytically active mRNA decapping enzyme located in specific cytoplasmic structures. *EMBO J* 21(24):6915–6924.
41. Song M-G, Li Y, Kiledjian M (2010) Multiple mRNA decapping enzymes in mammalian cells. *Mol Cell* 40(3):423–432.
42. Li Y, Song MG, Kiledjian M (2008) Transcript-specific decapping and regulated stability by the human Dcp2 decapping protein. *Mol Cell Biol* 28(3):939–948.
43. Li Y, Dai J, Song M, Fitzgerald-Bocarsly P, Kiledjian M (2012) Dcp2 decapping protein modulates mRNA stability of the critical interferon regulatory factor (IRF) IRF-7. *Mol Cell Biol* 32(6):1164–1172.
44. Li Y, Song M, Kiledjian M (2011) Differential utilization of decapping enzymes in mammalian mRNA decay pathways. *RNA* 17(3):419–428.
45. Tritschler F, et al. (2009) DCP1 forms asymmetric trimers to assemble into active mRNA decapping complexes in metazoa. *Proc Natl Acad Sci USA* 106(51):21591–21596.
46. Bouloy M, Pardigon N, Vialat P, Gerbaud S, Girard M (1990) Characterization of the 5′ and 3′ ends of viral messenger RNAs isolated from BHK21 cells infected with Germiston virus (Bunyavirus). *Virology* 175(1):50–58.
47. Hirsch CA, Hiatt HH (1966) Turnover of liver ribosomes in fed and in fasted rats. *J Biol Chem* 241(24):5936–5940.
48. Lam YW, Lamond AI, Mann M, Andersen JS (2007) Analysis of nucleolar protein dynamics reveals the nuclear degradation of ribosomal proteins. *Curr Biol* 17(9):749–760.
49. Jouffe C, et al. (2013) The circadian clock coordinates ribosome biogenesis. *PLoS Biol* 11(1):e1001455.
50. Huch S, Nissan T (2014) Interrelations between translation and general mRNA degradation in yeast. *Wiley Interdiscip Rev RNA* 5(6):747–763.
51. Won S, Ikegami T, Peters CJ, Makino S (2007) NSm protein of Rift Valley fever virus suppresses virus-induced apoptosis. *J Virol* 81(24):13335–13345.
52. Chawla-Sarkar M, et al. (2003) Apoptosis and interferons: Role of interferon-stimulated genes as mediators of apoptosis. *Apoptosis* 8(3):237–249.
53. Gil J, Esteban M (2000) Induction of apoptosis by the dsRNA-dependent protein kinase (PKR): Mechanism of action. *Apoptosis* 5(2):107–114.
54. Moon SL, Barnhart MD, Wilusz J (2012) Inhibition and avoidance of mRNA degradation by RNA viruses. *Curr Opin Microbiol* 15(4):500–505.
55. Reineke LC, Lloyd RE (2013) Diversion of stress granules and P-bodies during viral infection. *Virology* 436(2):255–267.
56. Emara MM, Brinton MA (2007) Interaction of TIA-1/TIAR with West Nile and dengue virus products in infected cells interferes with stress granule formation and processing body assembly. *Proc Natl Acad Sci USA* 104(21):9041–9046.
57. Chahar HS, Chen S, Manjunath N (2013) P-body components LSM1, GW182, DDX3, DDX6 and XRN1 are recruited to WNV replication sites and positively regulate viral replication. *Virology* 436(1):1–7.
58. Pager CT, Schütz S, Abraham TM, Luo G, Sarnow P (2013) Modulation of hepatitis C virus RNA abundance and virus release by dispersion of processing bodies and enrichment of stress granules. *Virology* 435(2):472–484.
59. Kwong AD, Kruper JA, Frenkel N (1988) Herpes simplex virus virion host shutoff function. *J Virol* 62(3):912–921.
60. Rowe M, et al. (2007) Host shutoff during productive Epstein-Barr virus infection is mediated by BGLF5 and may contribute to immune evasion. *Proc Natl Acad Sci USA* 104(9):3366–3371.
61. Glaunsinger B, Ganem D (2004) Lytic KSHV infection inhibits host gene expression by accelerating global mRNA turnover. *Mol Cell* 13(5):713–723.
62. Kamitani W, et al. (2006) Severe acute respiratory syndrome coronavirus nsp1 protein suppresses host gene expression by promoting host mRNA degradation. *Proc Natl Acad Sci USA* 103(34):12885–12890.
63. Cheng E, Mir MA (2012) Signatures of host mRNA 5′ terminus for efficient hantavirus cap snatching. *J Virol* 86(18):10173–10185.
64. Ptushkina M, et al. (1998) Cooperative modulation by eIF4G of eIF4E-binding to the mRNA 5′ cap in yeast involves a site partially shared by p20. *EMBO J* 17(16):4798–4808.
65. Mir MA, Panganiban AT (2008) A protein that replaces the entire cellular eIF4F complex. *EMBO J* 27(23):3129–3139.
66. Tsalikis J, Croitoru DO, Philpott DJ, Girardin SE (2013) Nutrient sensing and metabolic stress pathways in innate immunity. *Cell Microbiol* 15(10):1632–1641.
67. Brunton J, Steele S, Ziehr B, Moorman N, Kawula T (2013) Feeding uninvited guests: mTOR and AMPK set the table for intracellular pathogens. *PLoS Pathog* 9(10): e1003552.
68. Carpenter S, Ricci EP, Mercier BC, Moore MJ, Fitzgerald KA (2014) Post-transcriptional regulation of gene expression in innate immunity. *Nat Rev Immunol* 14(6):361–376.
69. Morita M, et al. (2013) mTORC1 controls mitochondrial activity and biogenesis through 4E-BP-dependent translational regulation. *Cell Metab* 18(5):698–711.
70. Moser TS, Jones RG, Thompson CB, Coyne CB, Cherry S (2010) A kinome RNAi screen identified AMPK as promoting poxvirus entry through the control of actin dynamics. *PLoS Pathog* 6(6):e1000954.
71. Petersen J, et al. (2014) The major cellular sterol regulatory pathway is required for Andes virus infection. *PLoS Pathog* 10(2):e1003911.
72. Filone CM, et al. (2010) Rift valley fever virus infection of human cells and insect hosts is promoted by protein kinase C epsilon. *PLoS One* 5(11):e15483.
73. Rose PP, et al. (2011) Natural resistance-associated macrophage protein is a cellular receptor for sindbis virus in both insect and mammalian hosts. *Cell Host Microbe* 10(2):97–104.
74. Cherry S, et al. (2005) Genome-wide RNAi screen reveals a specific sensitivity of IRES-containing RNA viruses to host translation inhibition. *Genes Dev* 19(4):445–452.
75. Xu J, et al. (2012) Transcriptional pausing controls a rapid antiviral innate immune response in *Drosophila*. *Cell Host Microbe* 12(4):531–543.